Supporting Information for:

Optical sensing of aqueous nitrate anion by a platinum(II) triimine salt based solid state material

Amie E. Norton,[‖,†*] Mahmood K. Abdolmaleki,[‖,‖] Logan Andriot,[‖] Christina Cashen,[‖] Jeanette A. Krause,[‖] William B. Connick[‖†] and Sayandev Chatterjee[ǂ*]
[‖]Department of Chemistry, University of Cincinnati, Cincinnati, OH 45221, United States of America
[†]Present address: Department of Entomology, Kansas State University, Manhattan, KS 66503, United States of America
[‖]Present address: Department of Biology and Chemistry, Texas A&M International University, Laredo, TX, 78041, United States of America
[ǂ]TerraPower LLC, Bellevue, WA 98008, United States of America
Email: amien@ksu.edu, schatterjee@terrapower.com

[†]This work is dedicated to William B. Connick, who passed away in April 2018

Table of Contents

EXPERIMENTAL

Reagents and Materials.

K_2PtCl_4 was purchased from Pressure Chemical. COD (1,5-cyclooctadiene), Cl-4-tpy (4-chloro-2,2′:6′2″-terpyridine) was obtained from Alfa Aesar. KBr, KCl, K_2SO_4, NaI, Na_2CO_3, $NaNO_3$, $NaClO_4$, KIO_4, $NaHCO_3$, and all solvents used were obtained from Sigma Aldrich. NH_4PF_6 was purchased from Alfa Aesar. Controlled Pore Glass (CPG) beads (383 Å pore size) were purchased from Prime Synthesis (Ashton, PA) and used as encapsulation supports.

1•Cl: **1**•Cl was prepared via published procedures.[1] In brief, **1**•Cl was synthesized by refluxing $Pt(COD)Cl_2$ (0.05 grams) and Cl-4-tpy (0.05 grams) in water (250 mL) for 12 hours. Slow evaporation of the solution generated crystals of **1**•Cl. The purities of the product were verified using a combination of ^1H nuclear magnetic resonance (NMR) spectroscopy and electrospray ionization mass spectrometry.

1•ClO_4: **1**•ClO_4 was prepared by modification of a literature procedure for the preparation of similar salts.[2,3] Briefly, the salt was generated by the metathesis of aqueous solution of **1**•Cl (0.05 g in 20 mL) with $NaClO_4$ (0.05 g) to generate a yellow precipitate. The salt was crystallized via slow evaporation from a 1:1 water:acetone solution.[2,3] The product was analyzed using a combination of ^1H NMR spectroscopy, electrospray ionization mass spectrometry, elemental analysis and single crystal X-ray diffraction.

^1H NMR (400 MHz, DMSO-d_6, δ): 8.9 (2 H), 8.7 (4 H, d), 8.55 (2H, t), 8.0 (2H, t).
MS-ESI (positive ion mode, CH_3CN) (m/z) : 497.9884 ($Pt(Cl\text{-}4\text{-}tpy)Cl^+$).
MS-ESI (negative ion mode, CH_3CN) (m/z) : 98.9386 (ClO_4^-)
X-Ray Powder Diffraction of bulk material matches single crystal (Figure S2)
Elemental analysis : Expected : C, 30.71 ; H, 1.69 ; N, 7.03 ; Found : C, 30.68 ; H, 1.49 ; N, 6.82

1•NO_3•$2H_2O$: **1**•NO_3•$2H_2O$ was prepared using a literature procedure.[4,5] In brief, 0.05 grams of **1**•Cl was dissolved in 1M HNO_3:acetone (1:1). Orange crystals of **1**•NO_3•$2H_2O$ precipitated out of the mixture. The product was analyzed using a combination of ^1H NMR spectroscopy, electrospray ionization mass spectrometry, elemental analysis and single crystal X-ray diffraction.

^1H NMR (400 MHz, DMSO-d_6, δ): 8.9 (4H), 8.7 (2H, d), 8.55 (2H, t), 8.0 (2H, t)
MS-ESI (positive ion mode, CH_3CN) (m/z): 497.9884 ($Pt(Cl\text{-}4\text{-}tpy)Cl^+$).
MS-ESI (negative ion mode, CH_3CN) (m/z): 61.9873 (NO_3^-)
X-Ray Powder Diffraction of bulk material matches single crystal (figure S2)
Elemental analysis: Expected : C, 30.21; H, 2.37; N, 9.40; Found : C, 30.01; H, 1.99; N, 9.11

CPGs impregnated with **1**•ClO_4 (**1**•ClO_4@CPG-383) or **1**•NO_3•$2H_2O$ (**1**•NO_3•$2H_2O$@CPG-383) were prepared from a 2 wt% solution of the respective complexes in a 1:1 mixture of acetone:DMSO. The solution was sonicated for 30 min and 0.5 mL was added to 0.1 g of the CPGs. The resultant **1**•ClO_4@CPG-383 and **1**•NO_3•$2H_2O$@CPG-383 were dried for 12 hours at 160°C.

For interference and sensitivity studies in complex multicomponent matrices, groundwater collected from the well 299-W19-36 at the nuclear waste site in Hanford, Washington was used for subsequent validation. The major inorganic constituents present in the groundwater are listed in Table S1,[6] among which NO_3^- has been reported as one of the dominant components (a concentration of 5.11×10^{-3} M reported and validated by ion chromatography measurements). For leaching experiments, measured amounts of CPGs loaded with both yellow and red of Pt(II) triimine salts were placed in DI water. The supernatant was monitored periodically using UV-visible spectroscopy.

Table S1. Major contaminants present in well 299-W19-36 at the Hanford site in Washington. Reproduced with permission from[6] Copyright 2016 the Royal Society of Chemistry.

Constituent	Concentration (µg/L)	Molarity (M)
Barium	113	8.23×10^{-7}
Calcium	122000	3.04×10^{-3}
Chloride	181000	5.11×10^{-3}
Total Cr	17.3	3.33×10^{-7}
Cr(VI)	0.05	9.62×10^{-10}
Magnesium	36400	1.50×10^{-3}
Molybdenum	65.9	6.87×10^{-7}
Nitrate	317000	5.11×10^{-3}
Potassium	7010	1.79×10^{-4}
Sodium	118000	5.13×10^{-3}
Sulfate	50000	5.21×10^{-4}
Strontium	618	7.05×10^{-6}
Tin	216	1.82×10^{-6}
Alkalinity ($CaCO_3$)	116000	1.16×10^{-3}
Uranium	174	7.31×10^{-7}

Characterization and Methods.

^{1}H NMR spectra were recorded at room temperature using a Bruker AC 400 MHz instrument. Deuterated solvents, tetramethylsilane, d_6-DMSO, D_2O and CD_3CN were all purchased from Cambridge Isotope Laboratories. Mass spectra were obtained by electrospray ionization of sample solutions using a Micromass Q-TOF-2 instrument.

Room-temperature steady-state emission spectra were collected using a SPEX Fluorolog-3 fluorimeter equipped with a double emission monochromator and a single excitation monochromator. Laser power was reduced to 0.1 mW using a neutral density filter. For single crystal emission measurements, single crystals of **1**•ClO_4 or **1**•NO_3•$2H_2O$ were mounted on a greased slide and placed in a cell. Uncorrected emission spectra were collected by exciting the sample at 436 nm. Powder diffractions were recorded using a Panalytical PXRD instrument while measurements on impregnated-CPG samples were performed using a Bruker D2 PHASER diffractometer (Cu Kα radiation, 1.54184 Å).

Scanning electron microscopy (SEM) analysis and energy dispersive spectroscopy (EDS) were performed using an FEI Quanta 3DFEG Dual Beam microscope operated at 10–20 kV. The samples were prepared by dispersing the sample particles onto carbon tape and coated with ∼5 nm of carbon to minimize charge effects. Compositional analysis was performed using an Oxford 80 mm2 SDD EDS detector. For quantitative EDS analysis, calculated K factors provided by INCA software were used. No correction for absorption within the specimen was performed.

For transmission electron microscopy (TEM) analyses, the samples were analyzed on an FEI Titan 80–300 kV transmission electron microscope operated at 300 kV. The microscope is equipped with a CEOS aberration corrector for the probe-forming lens, which allows imaging in scanning mode with sub-ångstrom resolution. Images were acquired on a high angle annular dark field (HAADF) detector. The detection angle was kept 3 times higher than the probe convergence angle of 18 mrad.

For examining colorimetric changes, **1**•ClO_4 powder (100 mg) was exposed to 10 mL of 0.1 M NO_3^- for 15 min before proceeding with data collection and analysis. For testing interferences from other anions, both **1**•ClO_4 powders and **1**•ClO_4@CPG-383 were used. For testing powder samples, **1**•ClO_4 powders were dissolved into acetone to make a 2% solution. Q-tips were dipped in the loading solution for 5 mins and then dried for 4 h prior to exposing them to various anions. The Q-tips were separately exposed, for 1 h, to aqueous solutions containing 1.0 M aqueous solutions of I^-, IO_3^-, BrO_3^-, Cl^-, PO_4^{3-}, SO_4^{2-}, CO_3^{2-}, and Br^-. For CPG testing, 2 g of CPGs were loaded with 2% of **1**•ClO_4 and separately exposed, for 1 h, to 1 mL of aqueous solutions containing 1.0 M I^-, IO_3^-, BrO_3^-, Cl^-, PO_4^{3-}, SO_4^{2-}, CO_3^{2-}, and Br^-. The emission intensities (λ_{ex} = 532 nm) of the exposed CPGs were compared to CPGs exposed to 10^{-4} M NO_3^- for the same time duration.

For measurements on Hanford groundwater, CPGs were loaded with 2 wt% mixture of **1**•ClO_4 from acetone solution. For limit of detection and limit of quantification measurements for in DI water and Hanford groundwater, the error bars are obtained from standard deviations based on three independent measurements.

Crystal Structure Determination[7]

Yellow needle-shaped crystals of **1**•ClO_4 were grown from acetone. Orange-red needles of **1**•NO_3•$2H_2O$ were grown from acetone-HNO_3. For X-ray examination and data collection, suitable crystals were mounted in a loop with Paratone-N oil and transferred to the goniostat bathed in a cold nitrogen stream. Intensity data for both complexes were collected at 150K on a Bruker PHOTON100 CMOS detector at Beamline 11.3.1 at the Advanced Light Source (Lawrence Berkeley National Laboratory) using synchrotron radiation tuned to λ=0.7749Å. The data frames were collected using the program APEX2 and processed using the program SAINT routine within APEX2. The data were corrected for absorption and beam corrections based on the multi-scan technique as implemented in SADABS.

The structures were solved by a combination of direct methods in SHELXTL and the difference Fourier technique and refined by full-matrix least squares on F^2. Non-hydrogen atoms were refined with anisotropic displacement parameters. The ClO_4^- oxygen atoms are heavily disordered, a multi-component disorder model (including O-atom displacement restraints) was applied. The H-atoms for both complexes were calculated and treated with a riding model. The H-atom isotropic displacement parameters were defined as a*U_{eq} of the adjacent atom (a = 1.5 for the solvent and 1.2 for the cation). **1**•NO_3•$2H_2O$ crystallizes as a dihydrate. H1W, H2W on the solvent oxygen were located from the difference map whereas H3W, H4W were calculated based on H-bonding interactions. The refinement converged with crystallographic agreement factors summarized in Table S2. The structure of the cations are shown in Figure S1 while selected cation distances and angles are summarized in Table S3. The Cl-O distances for the disordered ClO_4^- anion fall in the 1.386-1.515Å range. The N-O distances for the NO_3^- anion fall in the 1.386-1.515Å range. Hydrogen-bonding interactions for **1**•NO_3•$2H_2O$ are listed in Table S4.

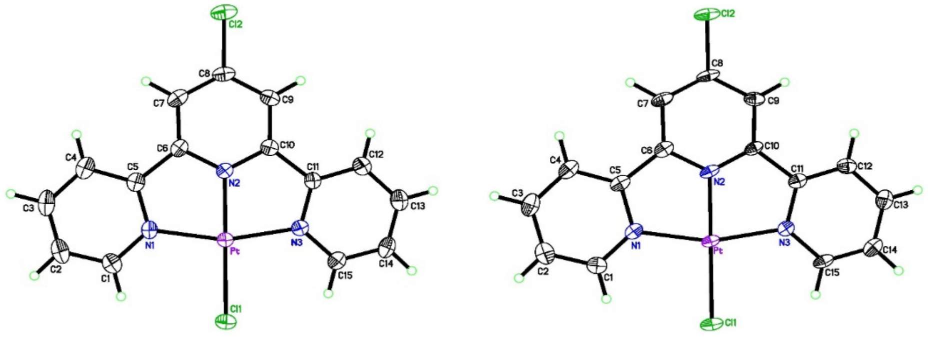

Figure S1. Structure of the cation for 1•ClO_4 (left) and **1**•NO_3•$2H_2O$ (right) at 50% ellipsoid probability and atomic numbering scheme

Table S2. Crystal data for red and yellow forms of **1**•ClO_4 and **1**•NO_3•$2H_2O$

	1•ClO_4	**1**•NO_3•$2H_2O$
CCDC deposition no.	CCDC-2170160	CCDC-2170168
Formula	$[C_{15}H_{10}N_3Cl_2Pt]ClO_4$	$[C_{15}H_{10}N_3Cl_2Pt]NO_3.2H_2O$
Formula wt	597.70	596.29
Temperature, K	150(2)	150(2)
Wavelength, Å	0.7749	0.7749 Å
Crystal system	Orthorhombic	Monoclinic
Space group	Pnma	$P2_1/n$
a, Å	16.1376(12)	11.6779(11)
b, Å	6.6715(5)	6.7449(7)
c, Å	15.6523(12)	23.025(2)
α, °	90	90
β, °	90	103.299(2)
γ, °	90	90
Volume, $Å^3$	1685.2(2)	1764.9(3)
Z	4	4
ρ_{calcd}, Mg/m^3	2.356	2.244
Crystal size, mm^3	0.040 x 0.020 x 0.020	0.270 x 0.005 x 0.005
θ range for data collection, °	2.752 to 31.138	2.386 to 31.223
Reflns collected/Indep. Reflns	33604 / 2263	22214 / 4406
R_{int}	0.0406	0.0390
Max./min. transmission	0.971 and 0.844	0.928 and 0.783
Data/restraints/parameters	2263 / 42 / 190	4406 / 0 / 244
Goodness-of-fit (S) on F^2	1.079	1.019
R, wR2 [$I>2\sigma(I)$]	0.0175, 0.0438	0.0196, 0.0402
R, wR2 [all data]	0.0200, 0.0448	0.0340, 0.0445

Table S3. Selected bond distances (Å) and angles (°) for **1**•ClO_4 and **1**•NO_3•$2H_2O$

	1•ClO_4	**1**•NO_3•$2H_2O$
Pt-N1 (Å)	2.013(3)	2.018(3)
Pt-N2 (Å)	1.933(3)	1.932(2)
Pt-N3 (Å)	2.013(3)	2.019(3)
Pt-Cl1 (Å)	2.2918(9)	2.2959(7)
N1-Pt-N2 (°)	81.38(13)	81.46(10)
N1-Pt-N3 (°)	162.49(13)	162.39(10)
N2-Pt-N3 (°)	81.11(13)	80.93(10)
N2-Pt-Cl1 (°)	179.97(9)	179.86(8)
Intermolecular Pt•••Pt Stacking Interactions		
Pt•••Pt_1 (Å)	4.1692(3)	3.3570(4)
Pt•••Pt_2 (Å)	4.1692(3)	3.4018(4)
Pt_1•••Pt•••Pt_2 (°)	106.28(1)	172.66(1)

Table S4. Hydrogen-Bonded Interactions for **1**•NO_3•$2H_2O$**:**

	d(D-H), Å	d(H•••A), Å	d(D•••A), Å	<(DHA), °
O(1W)-H(1W)...O(3)	0.88	2.12	2.942(5)	155.2
O(2W)-H(3W)...O(2)	0.89	1.92	2.805(4)	178.0
O(1W)-H(2W)...O(2W)#1	0.91	1.85	2.734(4)	163.0
O(2W)-H(4W)...O(1W)#2	0.89	1.89	2.774(5)	179.6

Symmetry transformations used to generate equivalent atoms: #1 x,y-1,z #2 -x+1/2,y+1/2,-z+3/2

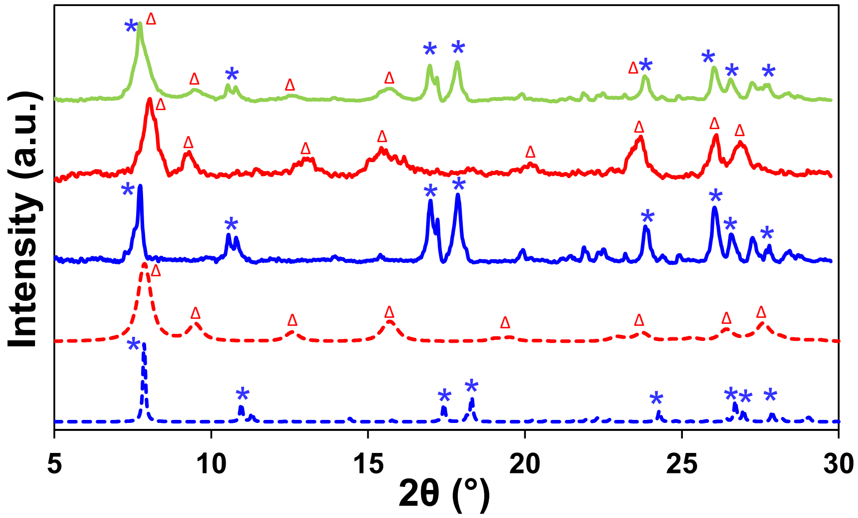

Figure S2. X-ray powder diffractograms: (bottom dashed blue line) simulated **1**•ClO_4 diffraction obtained from crystal structure, (second from bottom dashed red line) simulated **1**•NO_3•$2H_2O$ diffraction obtained from crystal structure, (middle solid blue line) experimental diffractogram from powder yellow **1**•ClO_4 samples, (second from top solid red line) experimental diffractogram from powder orange red **1**•NO_3•$2H_2O$ samples, (top solid green trace) **1**•ClO_4 post exposure to aqueous NO_3^- for 1 hour. "*" represents diffraction lines corresponding to pristine yellow **1**•ClO_4 while "Δ" represents diffraction lines corresponding to pristine orange red **1**•NO_3•$2H_2O$.

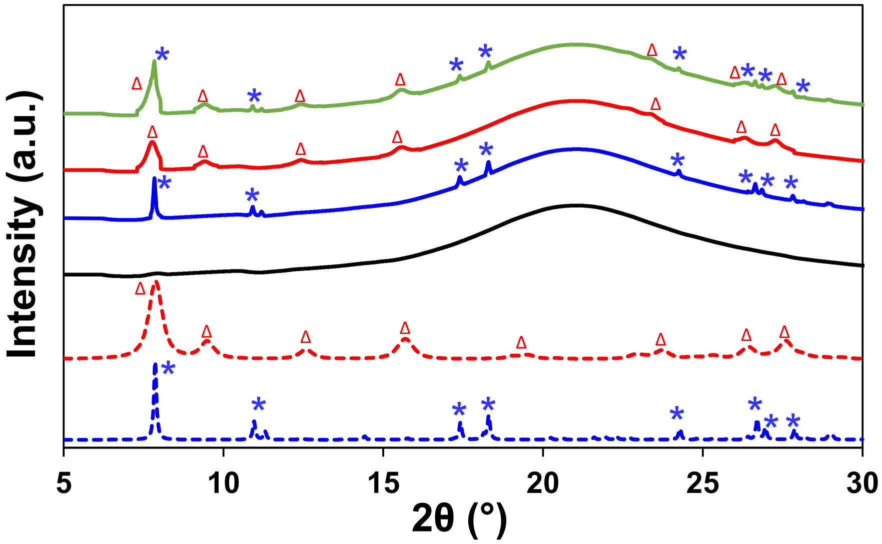

Figure S3. X-ray powder diffractograms of **1**•ClO_4@CPGs pre and post exposure to aqueous NO_3^-: (bottom dashed blue line) pristine yellow **1**•ClO_4, (second from bottom dashed red trace) pristine orange red **1**•NO_3•$2H_2O$, (third from bottom solid black line) blank CPG-383, (third from top solid blue line) **1**•ClO_4@CPG-383, (second from top solid red line) **1**•NO_3•$2H_2O$@CPG-383, (top solid green line) **1**•ClO_4@CPG-383 post exposure to aqueous NO_3^- for 1 hour. "*" represents diffraction lines corresponding to pristine yellow **1**•ClO_4 while "Δ" represents diffraction lines corresponding to pristine orange red **1**•NO_3•$2H_2O$.

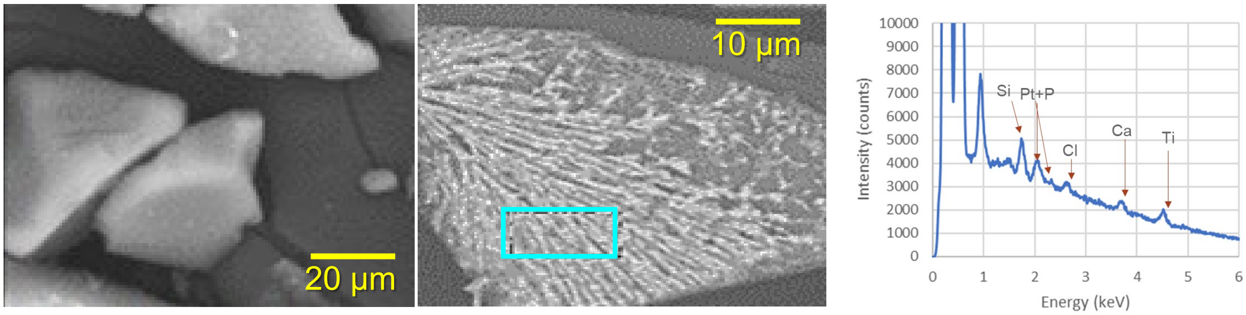

Figure S4. Representative SEM images of CPG-383 (left panel) and **1**•ClO_4@CPG-383 (middle panel, the light blue box represents the microcrystalline Pt(II) salt deposits on the surface of the CPG). (right panel) EDS profile of the blue box.

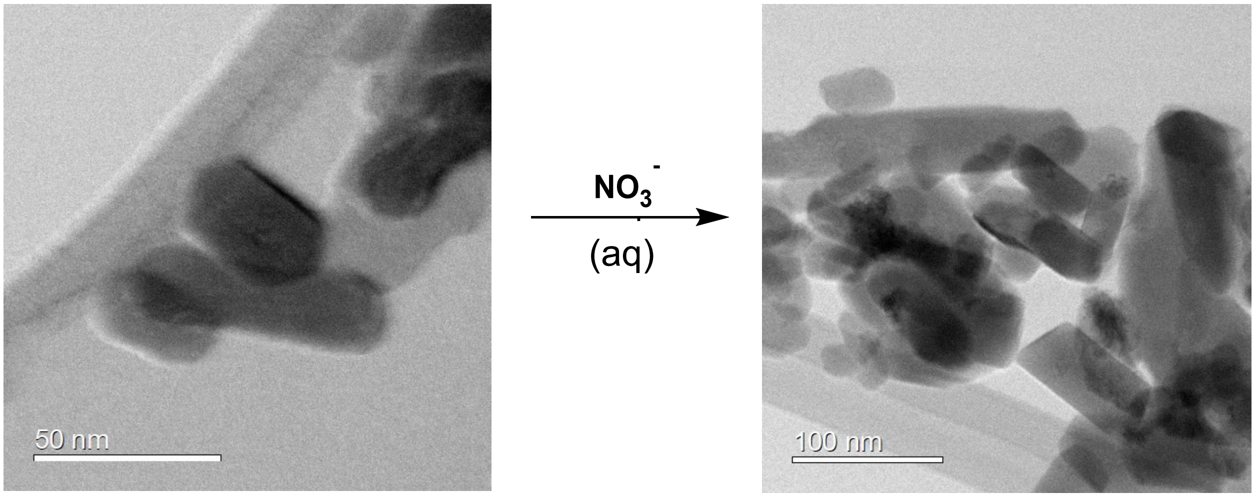

Figure S5. Representative TEM images of **1**•ClO_4@CPG-383 (left panel) and post exposure to aqueous 1M aqueous NO_3^- (right panel).

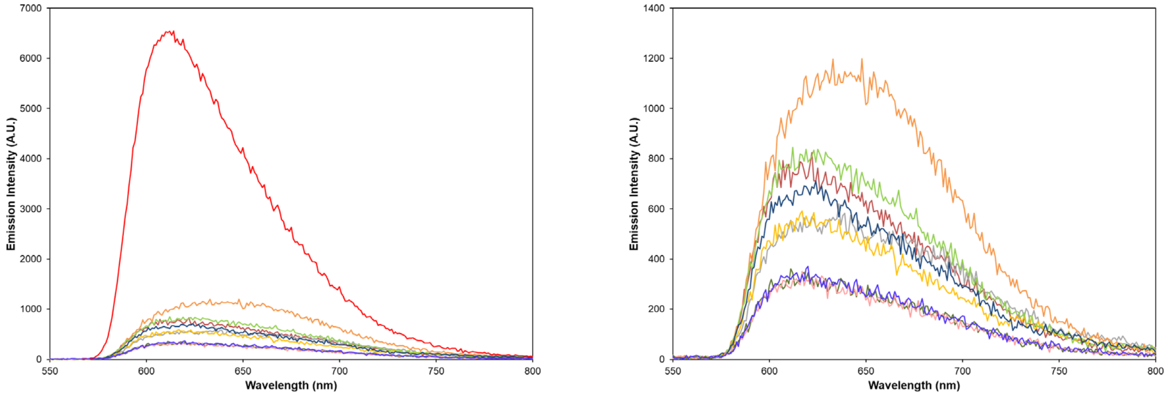

Figure S6. Response of **1**•ClO_4@CPG-383 to (—) 10^{-3} M NO_3^-, (—) 1.0 M F^-, (—) 1.0 M CO_3^{2-}, (—) 1.0 M SO_4^{2-}, (—) 0.1 M PO_4^{3-}, (—) 0.1 M ClO_4^-, (—) 0.1 M Cl^-, (—) 0.1 M BrO_3^-, (—) 0.1 M IO_3^-, (—) 0.1 M I^-; (Left panel with NO_3^-, Right panel without NO_3^-) (λ_{ex} = 532 nm).

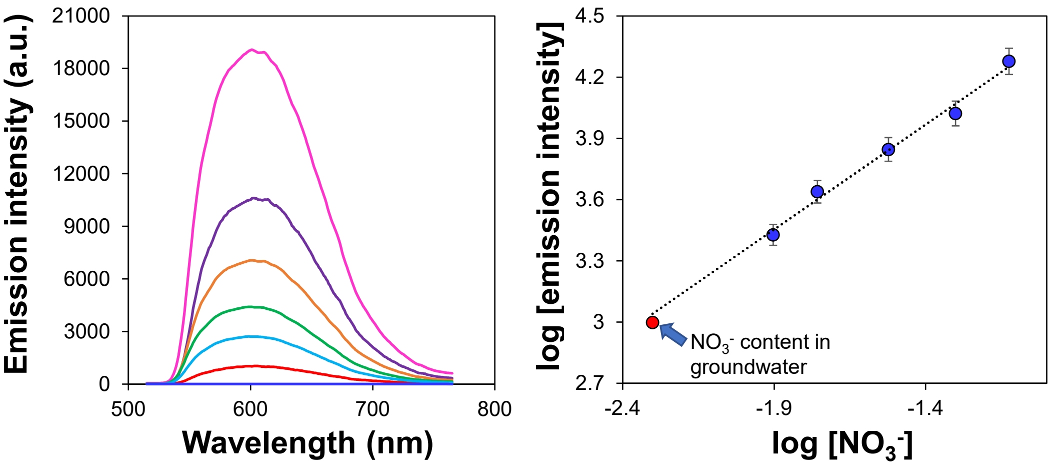

Figure S7. (left panel) Luminescence spectra of **1**•ClO_4@CPG-383 in presence of groundwater spiked with varying concentrations of NO_3^- for 1 hour (λ_{max} = 532 nm): (——) pristine **1**•ClO_4@CPG-383, (——) **1**•ClO_4@CPG-383 contacted with groundwater, (——) **1**•ClO_4@CPG-383 contacted with groundwater containing 1.25×10^{-2} M cumulative NO_3^-, (——) **1**•ClO_4@CPG-383 contacted with groundwater containing 1.75×10^{-2} M cumulative NO_3^-, (——) **1**•ClO_4@CPG-383 contacted with groundwater containing 2.49×10^{-2} M cumulative NO_3^-, (——) **1**•ClO_4@CPG-383 contacted with groundwater containing 4.97×10^{-2} M cumulative NO_3^-, (——) **1**•ClO_4@CPG-383 contacted with groundwater containing 7.51×10^{-2} M cumulative NO_3^-. (λ_{ex} = 532 nm) Groundwater was obtained from the well 299-W19-36 at the nuclear waste site in Hanford, Washington, USA. Each spectrum represents an average of three independent measurements; (right panel) log/log plot of the maximum emission intensity (λ_{max}= 611 nm) of **1**•ClO_4@CPG-383 versus the concentration of NO_3^- in solution. The equation of the line: log (emission intensity) = 1.03 log [NO_3^-] + 5.41, R^2 = 0.99. The error bars are obtained from standard deviations based on three independent measurements. The red symbol represents the groundwater sample.

Leaching studies.

Leaching studies performed on both the yellow **1**•ClO_4 and the red **1**•NO_3•$2H_2O$ salts @CPG upon prolonged contact with DI water, showed a 4-7% mass loss of the materials over 2 days indicated by optical spectroscopy. While the rate of loss is not significant in the context of rapid sensing applications, efforts are underway to understand and improve the salt retention into the CPG matrix.

References

1 P. Du, *Inorganica Chim. Acta*, 2010, **363**, 1355‑1358.

2 S. D. Taylor, W. Howard, N. Kaval, R. Hart, J. A. Krause and W. B. Connick, *Chem. Commun.*, 2010, **46**, 1070‑1072.

3 S. D. Taylor, A. E. Norton, R. T. Hart, M. K. Abdolmaleki, J. A. Krause and W. B. Connick, *Chem. Commun.*, 2013, **49**, 9161‑9163.

4 A. E. Norton, M. Sharma, C. Cashen, M.-A. Dourges, T. Toupance, J. A. Krause, R. K. Motkuri, W. B. Connick and S. Chatterjee, *ACS Appl. Mater. Interfaces*, 2021, **13**, 16197‑16209.

5 A. E. Norton, M. Karimi Abdolmaleki, J. Liang, M. Sharma, R. Golsby, A. Zoller, J. A. Krause, W. B. Connick and S. Chatterjee, *Chem. Commun.*, 2020, **56**, 10175‑10178.

6 S. Chatterjee, M. S. Fujimoto, Y. Du, G. B. Hall, N. Lahiri, E. D. Walter and L. Kovarik, *ACS Sens.*, 2020, **5**, 674‑685.

7 APEX2 v2014.11-0 and SAINT v8.34A, Bruker Analytical X-ray Instruments, Inc., Madison, WI; SADABS v2014.5, G.M. Sheldrick, University of Göttingen, Germany; SHELXTL v6.14 & SHELX 2014/7, G.M. Sheldrick, University of Göttingen, Germany & Bruker Analytical X-ray Instruments, Inc., Madison, WI; scattering factors for non-standard wavelengths, L. Kissel & R.H. Pratt, Acta Cryst A (1990), **A46**, 170-175.